JOURNAL OF INFORMATION, KNOWLEDGE AND RESEARCH IN ELECTRICAL ENGINEERING

TRANSIENT STABILITY ANALYSIS OF PV BASED MICROGRID WITH ESS

Vijay A
Department of Electrical and Electronics Engineering
Government College of Technology
Coimbatore
er.vijay45@gmail.com

Dr.E.Latha Mercy Ph.D
Associate Professor
Department of Electrical and Electronics Engineering
Government College of Technology
Coimbatore
mercy@gct.ac.in

Mohamed Abdul Kalam M
Department of Electrical and Electronics Engineering
Government College of Technology
Coimbatore
eeeabdul54@gmail.com

Ronald S.Ebenezer,
Department of Electrical and Electronics Engineering
PSG Tech
Coimbatore
Ronaldsebbenezer7@gmail.com

***Abstract*—**

Due to the seasonal availability and uneven distribution of the renewable energy sources, more emphasis is made to integrate microgrids with the energy storage systems to utilize power more effectively and efficiently with good power quality as well as reliability. In the proposed system the Superconducting Magnetic Energy Storage system (SMES) and Battery Energy Storage System (BESS) used to stabilize the PV based microgrid during transient conditions. SMES is efficient in providing short term instantaneous power due to its high power density and battery is good at supplying the long term continuous power due to its high energy density. Hence, the proposed system combines the complementary characteristics of SMES and battery to stabilize the PV based microgrid during transient conditions which is more techno economic to be applied in electric power grids. Comparative analysis is carried out with SMES-BESS and only with battery using MATLAB simulink.

Keywords— Superconducting Magnetic Energy Storage System(SMES), Battery Energy storage System(BESS), PV generation, microgrid.

I.INTRODUCTION

In the widely-focused energy storage systems, Superconducting Magnetic Energy Storage (SMES) and battery are two major systems [1], [2]. SMES is efficient at handling the short-term instantaneous power due to its high power density, fast transient response and discharging efficiency, and battery is also efficient in supplying the long-term continuous power due to its large energy density, and long cyclic life. Since they are complementary in their characteristics, it is recommended to form a SMES-battery Energy Storage System (ESS), which can be more techno-economic to be applied in electric power grids. In the research of SMES-battery application the literature review is carried out. In [3], a synergistic control approach is proposed for a SMES-battery to enable the dispatchability of renewable energy. In [4], the applications of a SMES-battery on adjusting the outputs of direct drive linear wave energy converters (DDLWEC) are addressed. In [5], [6], the battery lifetime extension, control methods of a SMES-battery have been proposed. In addition, it is found that using SMES-battery offers good contributions in the following research fields: a) the power buffer between PV energy systems and the main network [7]; b) the grid integration and output stabilization of wind generators [8], [9]; c) the fast charging of electric vehicles [10]; d) the electric bus [11]; e) the support of dynamic voltage restorer [12], [13]; f) the primary frequency control of an isolated microgrid [14].

In the literature review, it is obvious that SMES-battery has advantages in handling the power swing, energy transfer, voltage fluctuation and related transient stability issues. The existing control schemes and coordination methods can help to lay some theoretical foundations for the expanding applications of SMES-battery. In the interconnected microgrid which is accommodating more number of distributed renewable energy, a preliminary study on the integration of a SMES-battery into it has been conducted [15].

The existing systems do not systematically study how the SMES-battery responds to the microgrid's mode switching under different faults, and also they did not address the operational characteristics of the SMES magnet during its energy exchange with the microgrid. Aiming at the aforementioned tasks, this paper studies the utilization of a SMES-battery in a photovoltaic-based microgrid under external and internal faults. The modelling, control and coordination of the SMES-battery are stated. According to the MATLAB software, the transient behaviours of the microgrid under different faults are evaluated, and a comparison of with the SMES-battery and only with the battery is carried out

II. BASIC PRINCIPLE

Fig. 1 shows the application of a SMES-battery in a photovoltaic-based microgrid, which is composed of solar PV generator and load. The SMES and the battery are independently controlled, and a fully active topology Including the two DC/DC and DC-AC converters is adopted [16].

A. Battery

Battery is good at supplying the long-term continuous power due to its large energy density, and long cyclic life. During normal conditions the microgrid operates normally, the battery storage is utilized for the long-term power fluctuation (low-frequency power component) in the PCC. For the faults, the battery storage will act as a backup supply and coordinate with the SMES, and it is important when the SMES available capacity is insufficient.

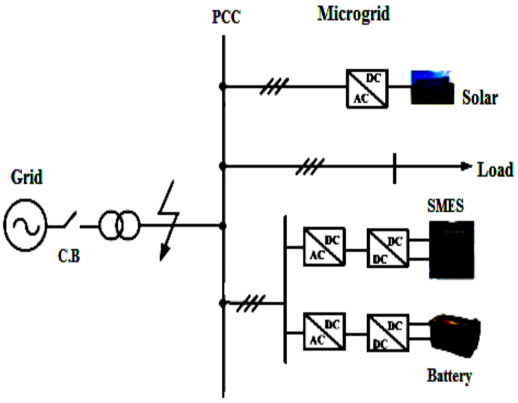

Fig. 1 Block diagram of PV based microgrid with SMES and battery

To ensure the coordination in the operation, the DC-AC inverter of the battery storage has the P-Q and V-F control modes.

B. *Superconducting Magnetic Energy Storage system (SMES)*

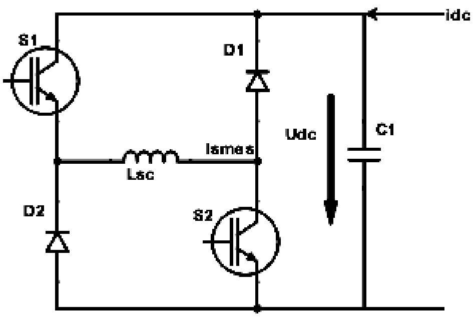

Fig. 2 Topology of the DC/DC chopper with the SMES magnet

Fig. 2 illustrates the typical topology of the DC/DC chopper integrated with the SMES magnet. In principle, the SMES's stored energy E_{SMES} and available power P_{SMES} are denoted as:

$$E_{SMES} = 0.5 L_{SC} I^2_{SMES}$$

$$P_{SMES} = \min\left(P_{ref\text{-}SMES}, U_{dc} I_{SMES}\right) \quad \text{……..(1)}$$

Where

L_{SC} is the magnet inductance
I_{SMES} is the magnet current
U_{dc} is the DC-link voltage
$P_{ref-SMES}$ is the power reference.

The effects of the SMES on the microgrid under different conditions are given by 1) When the microgrid normally operates and does an energy exchange with the grid, the SMES is used to alleviate the short-term power fluctuation in the PCC. 2) When the microgrid experiences an external fault, its islanded mode will be triggered, and SMES is used to control the microgrid's voltage and frequency for realizing a smooth mode transfer. 3) In case of an internal fault, the microgrid is expected to do a fault-ride-through (FRT) operation, and the SMES will adjust the power flow to limit the fault current in the PCC.

Fig. 3 shows the control block diagram of the SMES for the microgrid. In Fig. 3(a), the active and reactive power (P-Q) control is used to handle the normal case and the internal fault. In Fig. 3(b), the voltage and frequency (V-F) control is used to handle the external fault. Here, voltage outer-loop regulator and a current inner-loop regulator are used [19], and also the frequency adjustment based open-loop control is applied. It explains that the frequency reference after an integral processing will be sent to the Pulse-Width Modulation (PWM) as to make the SMES inverter's voltage outputs be controlled within a given frequency

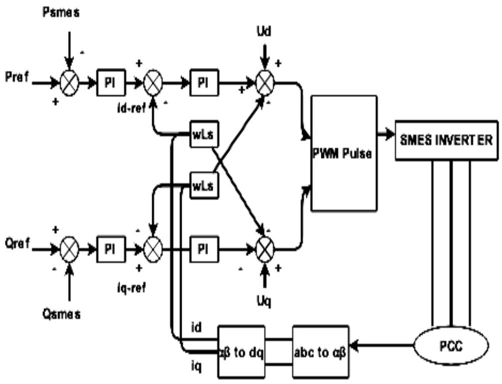

Fig. 3(a) Control block diagram for P-Q control mode

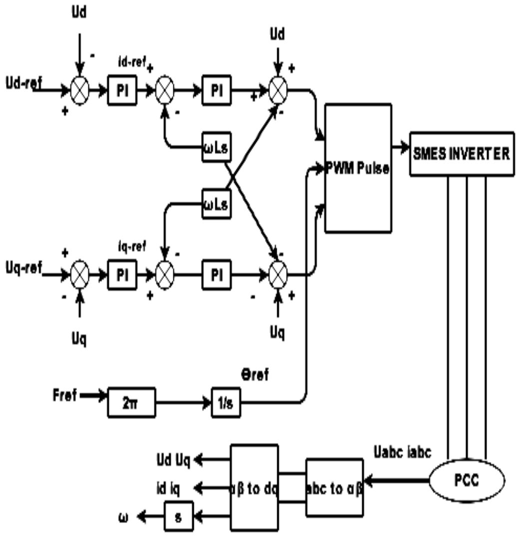

Fig. 3(b) Control block diagram for V-F control mode

C. *Coordination of SMES-battery*

For the coordination of the SMES and battery, the basic three modes are considered: 1) only using the SMES, 2) combined use of the SMES and the battery, 3) only using the battery. Here, the magnet current ISMES is selected as a critical factor to determine when the battery will play a role and the SMES will be out of service. The current coefficient '*α*' is introduced for evaluating the change of ISMES and calculating the criterions shown in the following tables.

Table I
COORDINATION OF SMES-BATTERY FOR THE INTERNAL FAULT

Criterions	Constant P-Q Control	
	SMES	Battery
$I_{SMES\text{-}max} \geq I_{SMES} \geq [I_{SMES\text{-}min} + \alpha(I_{SMES\text{-}max} - I_{SMES\text{-}min})]$	P_{ref} , Q_{ref}	0
$[I_{SMES\text{-}min} + \alpha(I_{SMES\text{-}max} - I_{SMES\text{-}min})] \geq I_{SMES} \geq I_{SMES\text{-}min}$	P_{ref} - P_b Q_{ref} - Q_b	P_b, Q_b
$I_{SMES} = I_{SMES\text{-}min}$	0	P_{ref} ,Q_{ref}

Table II
COORDINATION OF SMES-BATTERY FOR THE EXTERNAL FAULT

Criterions	Control mode selection	
	SMES	Battery
Normal condition(C.B closed)	P-Q	P-Q
$I_{SMES\text{-}max} \geq I_{SMES} \geq [I_{SMES\text{-}min} + \alpha(I_{SMES\text{-}max} - I_{SMES\text{-}min})]$ & C.B opened	V-F	P-Q
$[I_{SMES\text{-}min} + \alpha(I_{SMES\text{-}max} - I_{SMES\text{-}min})] \geq I_{SMES} \geq I_{SMES\text{-}min}$	V-F	V-F
$I_{SMES} = I_{SMES\text{-}min}$	P-Q	V-F

Table I shows that the SMES and the battery share the total power references (P_{ref}, Q_{ref}) during the internal fault. Here, the battery's references (P_b, Q_b) will be linearly increased with the decrease of the current I_{SMES}, and only, if the microgrid is connected to the grid, the P-Q control mode of the SMES-battery keeps working. It is important for the power sharing of the SMES and the battery to handle the microgrid's normal state fluctuation, a low-pass filter can be properly adopted to execute a primary arrangement, and a valid grading strategy for driving high-frequency and low-frequency power components can be effectively applied [10], [11].

During external fault, the transfer between the P-Q control and the V-F control is activated based on the PCC breaker (C.B) and the magnet current I_{SMES}, as shown in Table II. From this table, it is established that when the magnet current drops to a certain range, both the SMES and the battery will switch to the V-F control scheme at the same time, and the capacity requirements can be fully satisfied. In this case, it should be noted that, when the references of voltage and frequency for the SMES and the battery have a difference, the circulating current may be caused among them.

To prevent the flow of higher circulating current, it is necessary to decrease the time overlap for the SMES and the battery both with the V-F control and it can be achieved by controlling the switching time of the battery. The other solution is to introduce virtual impedance, and the control scheme improvement is helpful to strengthening the system's stable operation [22], [23].

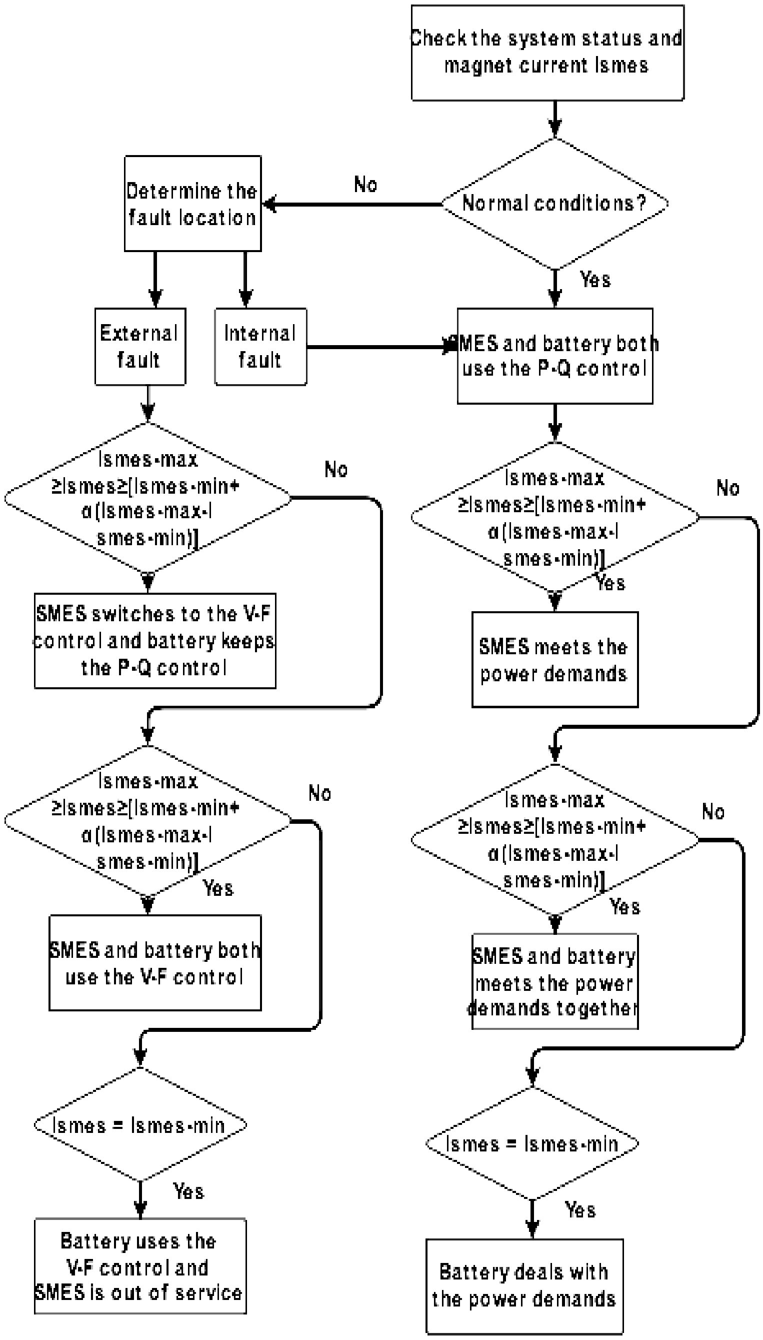

Fig. 4 Coordination method for the SMES-battery

III. PERFORMANCE EVALUATION

To evaluate the proposed system SMES-battery with the microgrid is simulated in MATLAB/Simulink. The proposed model is simulated for the microgrid meets different faults. Figure 6 shows the Simulation model for SMES-battery connected microgrid. In this MATLAB simulation, PV panel of 100kw is connected to the microgrid with energy storage system of Battery and SMES. PV panel has individual module rating of open circuit voltage of 36.3V and short circuit current of 7.84A, connected as 10 series string and 40 parallel strings to generate 100kw power. This DC power gets converted to AC through inverter circuit and connected to Point of Common Coupling (PCC). Constant voltage of 415V is maintained at PCC.

Two lithium-ion battery of rated 220VDC, 50AH is connected in series and the DC power is converted to AC through converter circuit and connected to the PCC of microgrid. SMES unit of chopper circuit is also connected to the PCC of microgrid through converter circuit. External grid supply 415V AC is connected to PCC of microgrid through switching unit. A 500W load is connected from PCC of micro grid. Simulation is done with SMES-battery connected microgrid and only battery connected microgrid for both external and internal fault conditions.

A. *Simulation for external fault conditions*

For external fault conditions, the simulation is done for SMES-battery with microgrid, and also for only battery connected with microgrid. Considering the fault occurs on grid side at t=0.4sec. Based on the SMES current ISMES the power sharing between the SMES and the battery is determined, and it is designed that when the SMES current reduces to 40% of its initial working current, the battery will battery continues to supply power to microgrid. Figure 6(a) Shows the power waveform at PCC during external fault conditions in the system connected with SMES and battery. And also figure 6(b) shows the voltage and current waveform at microgrid's PCC during the external fault conditions.

For the similar external fault conditions, the simulation is done for only battery connected microgrid. The power, voltage and current waveform at PCC is shown in figure. Figure 6(c) shows the power waveform at PCC during external fault conditions in the system connected with SMES and battery. And also figure 6(d) shows the voltage and current waveform at microgrid's PCC

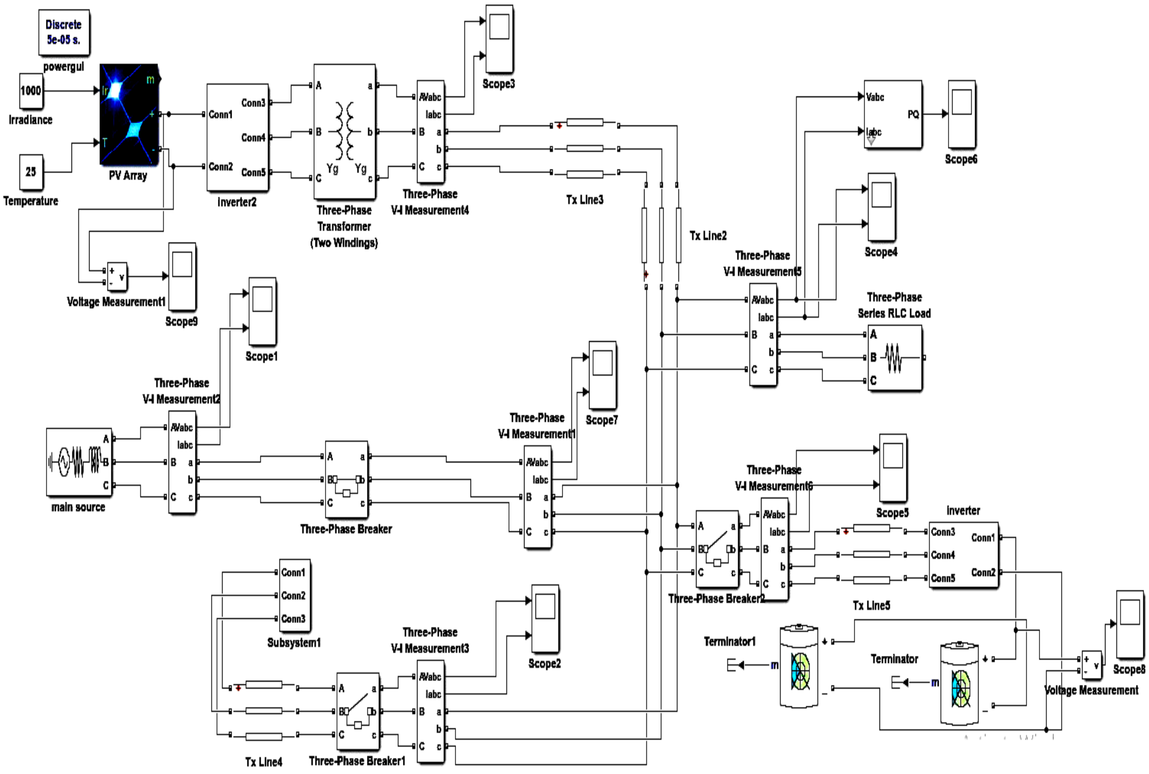

Fig. 6 Simulation model for SMES-battery connected microgrid

B. *Simulation for internal fault conditions*

For internal fault conditions, the simulation is done for SMES-battery with microgrid, and also for only battery connected with microgrid. The internal fault occurs on load at t=0.4sec. For the SMES-battery, the power fluctuation and the fault current in the PCC are restricted at the initial stage of the fault. For only with the battery, its fault response is slow and the power compensation requires a long transient process. It is observed from the simulation that the fault current with the battery is about 1.42 times of that with the SMES-battery. Thus, the SMES-battery is able to improve the microgrid's transient stability more effectively than the battery. The change of ISMES determines the power sharing between the SMES and the battery, and it is designed that when the SMES current reduces to 40% of its initial working current, the battery will completely replace the SMES. After the internal fault is removed, the grid starts to charge the SMES-battery, and for the SMES-battery, which may recover itself in time to play a role in subsequent operations.

The figure 7(a) shows the power response at PCC during internal fault conditions for SMES-battery connected microgrid and figure 7(b) illustrate power response at PCC during internal fault conditions for battery connected microgrid.

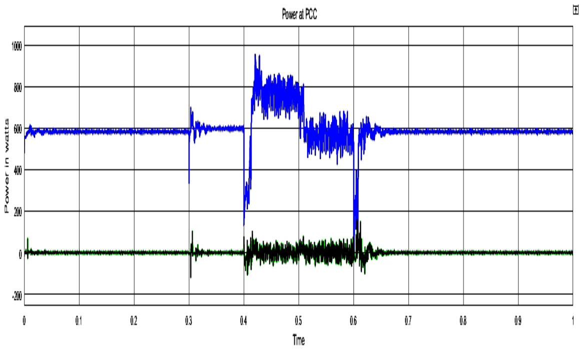

Fig. 6(a) Power response at PCC during external fault conditions for SMES-battery connected microgrid

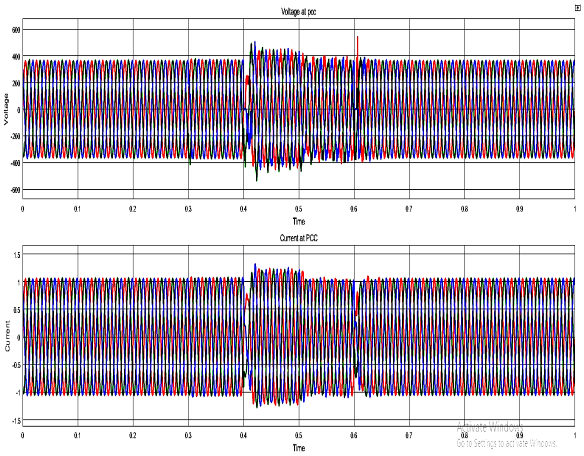

Fig. 6(b) voltage and current waveform at microgrid's PCC during the external fault conditions for SMES-battery connected microgrid

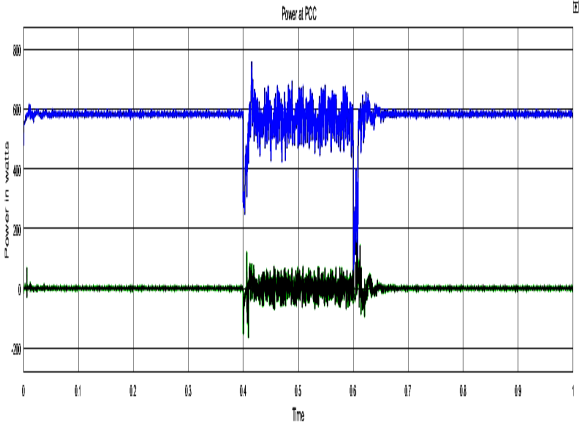

Fig. 6(c) Power response at PCC during external fault conditions for battery connected microgrid

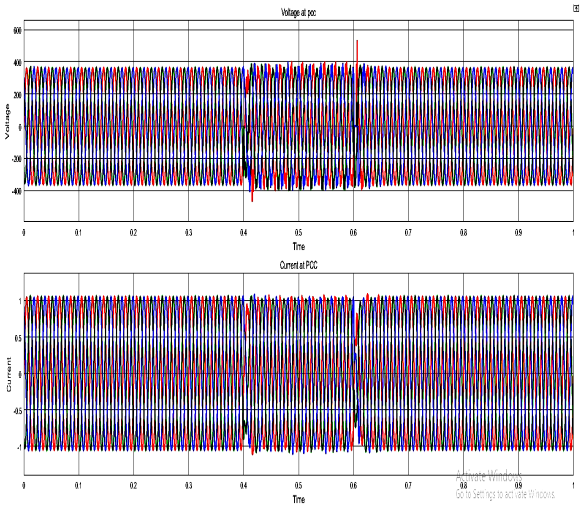

Fig. 6(d) voltage and current waveform at microgrid's PCC during the external fault conditions for battery connected microgrid

B. *Simulation for internal fault conditions*

For internal fault conditions, the simulation is done for SMES-battery with microgrid, and also for only battery connected with microgrid. The internal fault occurs on load at t=0.4sec. For the SMES-battery, the power fluctuation and the fault current in the PCC are restricted at the initial stage of the fault. For only with the battery, its fault response is slow and the power compensation requires a long transient process. It is observed from the simulation that the fault current with the battery is about 1.42 times of that with the SMES-battery. Thus, the SMES-battery is able to improve the microgrid's transient stability more effectively than the battery. The change of I_{SMES} determines the power sharing between the SMES and the battery, and it is designed that when the SMES current reduces to 40% of its initial working current, the battery will completely replace the SMES. After the internal fault is removed, the grid starts to charge the SMES-battery, and for the SMES-battery, which may recover itself in time to play a role in subsequent operations.

The figure 6(a) shows the power response at PCC during internal fault conditions for SMES-battery connected microgrid and figure 6(b) illustrate power response at PCC during internal fault conditions for battery connected microgrid.

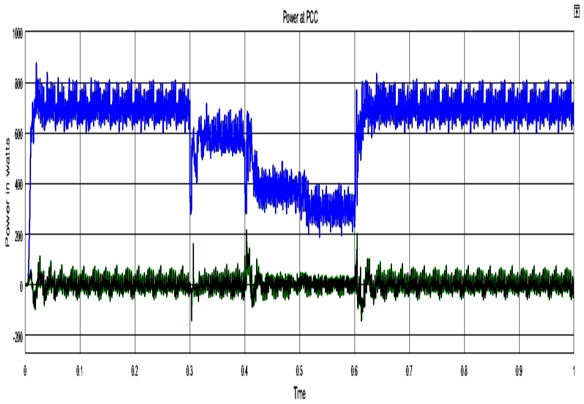

Fig. 7(a) Power response at PCC during internal fault conditions for SMES-battery connected microgrid

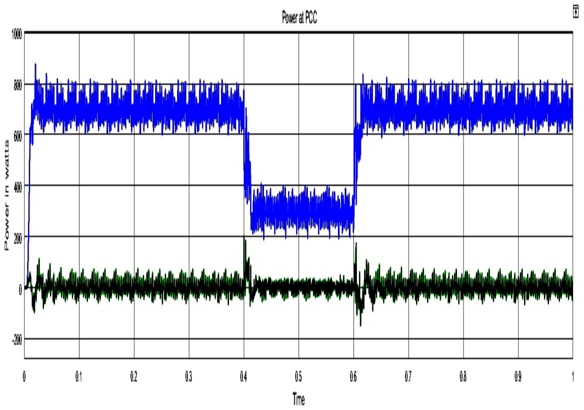

Fig. 7(b) Power response at PCC during internal fault conditions for battery connected microgrid

IV. CONCLUSION

In this proposed system, the SMES-battery ESS is used to improve the transient stability of a photovoltaic-based microgrid under different fault conditions. From the theoretical analysis and simulation verification it can be concluded that:

1) The SMES-battery is better than the battery to timely handle the transient fault issues of the microgrid. At the initial stage of the fault conditions, the SMES-battery is capable of offering a instantaneous power injection to the microgrid.

2) The SMES-battery is superior to the battery to ensure a smooth mode transition for the microgrid under the external fault, and reduce the fault current in the PCC to avoid an unnecessary off-grid under the internal fault.

.

REFERENCES

[1] M. Farhadi and O. Mohammed, “Energy storage technologies for highpower applications,” *IEEE Trans. Ind. Appl.*, vol. 52, no. 3, pp. 1953–1961, May 2016.

[2] X. Y. Chen and J. X. Jin, “Energy efficiency analysis and energy management of a superconducting LVDC Network,” *IEEE Trans. Appl. Superconduct.*, vol. 26, no. 7, Oct. 2016, Art. no. 5403205.

[3] J. W. Shim, Y. Cho, S.-J. Kim, S. W. Min, and K. Hur, “Synergistic control of SMES and battery energy storage for enabling dispatchabilityof renewable energy sources,” *IEEE Trans. Appl. Supercond.*, vol. 23,no. 3, Jun. 2013, Art. no. 5701205.

[4] Z. Nie, X. Xiao, Q. Kang, R. Aggarwal, H. Zhang, andW. Yuan, “SMESbattery energy storage system for conditioning outputs from direct drive linear wave energy converters,” *IEEE Trans. Appl. Supercond.*, vol. 23, no. 3, Jun. 2013, Art. no. 5000705.

[5] J. Li, A. M. Gee, M. Zhang, and W. Yuan, “Analysis of battery lifetime extension in a SMES-battery hybrid energy storage system using a novel battery lifetime model,” *Energy*, vol. 86, pp. 175–185, Jun. 2015.

[6] J. Li *et al.*, “Design and test of a new droop control algorithm for a SMES/battery hybrid energy storage system,” *Energy*, vol. 118, pp. 1110– 1122, Jan. 2017.

[7] Z. Wang, Z. Zou, and Y. Zheng, “Design and control of a photovoltaic energy and SMES hybrid system with current-source grid inverter,” *IEEE Trans. Appl. Supercond.*, vol. 23, no. 3, Jun. 2013, Art. no. 5701505.

[8] S.Wang *et al.*, “Design and advanced control strategies of a hybrid energy storage system for the grid integration of wind power generations,” *IET Renew. Power Gener.*, vol. 9, no. 2, pp. 89–98, 2015.

[9] X.Lin andY.Lei, “Coordinated control strategies for SMES-battery hybrid energy storage systems,” *IEEE Access*, vol. 5, pp. 23452–23465, Oct. 2017.

[10] J. Deng *et al.*, “Application of a hybrid energy storage system in the fast charging station of electric vehicles,” *IET Gener. Transm. Distrib.*, vol. 10, no. 4, pp. 1092–1097, Mar. 2016.

[11] J. Li, M. Zhang, Q. Yang, Z. Zhang, and W. Yuan, “SMES/battery hybrid energy storage system for electric buses,” *IEEE Trans. Appl. Supercond.*, vol. 26, no. 4, Jun. 2016, Art. no. 5700305.

[12] A. M. Gee *et al.*, “A superconducting magnetic energy storageemulator/battery supported dynamic voltage restorer,” *IEEE Trans. Energy Conver.*, vol. 32, no. 1, pp. 55–64, Mar. 2017.

[13] Z .-X. Zheng, X.-Y. Chen, X.-Y. Xiao, and C.-J. Huang, “Design and evaluation of a Mini-Size SMES magnet for hybrid energy storage

application in a kW-class dynamic voltage restorer," *IEEE Trans. Appl. Supercond.*, vol. 27, no. 7, Oct. 2017, Art. no. 5700911.

[14] J. Li, R. Xiong, Q. Yang, F. Liang, M. Zhang, and W. Yuan, "Design/test of a hybrid energy storage system for primary frequency control using a dynamic droop method in an isolated microgrid power system," *Appl. Energy*, vol. 201, pp. 257–269, Sep. 2017.

[15] A. Cansiz, C. Faydaci, M. Talha Qureshi, O. Usta, and D. T. McGuiness, "Integration of a SMES–battery-based hybrid energy storage system into microgrids," *J. Supercond. Novel Magn.*, Sep. 2017. [Online]. Available:https://doi.org/10.1007/s10948-017-4338-4

[16] Y. Kim, V. Raghunathan, and A. Raghunathan, "Design and management of battery-supercapacitor hybrid electrical energy storage systems for regulation services," *IEEE Trans. Multi-Scale Comput. Syst.*, vol. 3, no. 1, pp. 12–24, Jan.–Mar. 2017.